Energy for Sustainable Development 32 (2016) 1–13

Contents lists available at ScienceDirect

Energy for Sustainable Development

Evaluation of the efficiency of dual compound parabolic and involute concentrator

Abid Ustaoglu [a], Junnosuke Okajima [b], Xin-Rong Zhang [c], Shigenao Maruyama [b]

[a] Graduate School of Engineering, Tohoku University, Sendai 980-8577, Japan
[b] Institute of Fluid Science, Tohoku University, Sendai 980-8577, Japan
[c] Department of Energy and Resources Engineering, College of Engineering, Peking University, Beijing 100871, China

ARTICLE INFO

Article history:
Received 31 July 2014
Revised 26 January 2016
Accepted 11 February 2016
Available online xxxx

Keywords:
Compound parabolic reflector
Involute reflector
Evacuated tube
Ray tracing
Dual concentrator
Seasonal performance

ABSTRACT

A two-stage line axis solar thermal concentrator consisting of a compound parabolic and an involute reflector was designed, and its thermal and optical performance was compared with that of a dual concentrator. The configuration of the reflectors with tubular absorber yields the highest possible concentration and uniform temperature distribution on the absorber. To reduce the heat loss from the absorber, the concentrator was covered with evacuated glass tube. The dual concentrator increases ray acceptance, which is defined as the ratio of the reflector aperture area to the glass cover diameter; hence, the concentrator can utilize incident solar radiation more effectively with only a slight increase of 28% in the glass cover circumference. This suggests the use of dual concentrators in multiple concentrator units owing to their lower component cost. The performance was evaluated by using a ray-tracing model for two-dimensional (2D) geometry. The average optical efficiency of dual and single concentrators was 57% and 37%, respectively. The thermal efficiency of the dual concentrator was 21% higher than that of single one at the absorber temperature of 373 K for the gray surface absorber. On the other hand, the selective surface absorber significantly increased the performance, suggesting that the concentrator can be used in high-temperature applications such as steam generation. Annual and seasonal performances were analyzed as well. Assuming infinite length of the line-axis concentrator's absorber pipe allows ignoring the end effects; thus, a 2D approach was adopted. As a result, the dual concentrator showed better performance for all seasons; however, the solar utilization time of both concentrator types became shorter during the winter and summer solstices because of the weak insolation resulting from the orientation of the concentrators. Therefore, a slight seasonal adjustment or a modification of the geometry is required for longer utilization.

© 2016 International Energy Initiative. Published by Elsevier Inc. All rights reserved.

1. Introduction

The search for alternative sources of energy is driven by the significant increase in fuel price, limited fossil-fuel reserves, alarming rate of environmental pollution, and the increasing levels of greenhouse gas emission (Topkaya, 2012; Balat, 2009).

Solar energy is one of the cleanest alternative sources of energy that does not contribute to global warming (Solangi et al., 2011). Moreover, the yearly energy consumption by all humans is comparable to the amount of energy contained in solar radiation that reaches the Earth's surface in a period of 1 h; hence, solar energy is the most plentiful of the alternative energy types (IEA, 2010). Solar energy has been used for decades in industrial and commercial sectors. Several different solar energy collection technologies have been developed, such as solar collectors.

Solar collectors are a special class of heat exchangers that convert solar radiation energy into heat or directly into electric energy. Solar collectors can be further classified into two categories as non-concentrating and concentrating collectors based on their concentration ratios. Non-concentrating collectors have concentration ratio of 1, implying that the intercepting area is equal to the absorbing area. In general, non-concentrating collectors are more feasible for use in low-temperature applications related to low heat flux. Many studies have been conducted on non-concentrating collectors (Khoukhi and Maruyama, 2005; Khoukhi et al., 2006). On the other hand, in the solar concentrating collectors, lenses or mirrors and tracking systems are used to concentrate the incident solar radiation in a much smaller receiving area. For a system that operates at high temperature, the thermodynamic cycle can achieve a higher Carnot efficiency as a result of the increased heat flux (Kalogirou, 2004; Tian and Zhao, 2013).

A specific collector concept or design can find a market niche if it has promising durability, cost efficiency, and effective performance. Many existing collector systems do not satisfy these requirements. Collector performance decreases due to the aging of its optical components (especially, the reflector and absorber), and environmental factors such as dust and climate variation promote this performance reduction (Nostell et al., 1998; Kaltenbach et al., 2012). Moreover, reflector's surface must be kept clean to avoid performance deterioration. However, some solar systems with uncovered absorbers might be difficult to maintain and clean owing to high absorber temperature. A non-uniform illumination of the absorber can yield occasional hot spots of

http://dx.doi.org/10.1016/j.esd.2016.02.007
0973-0826/© 2016 International Energy Initiative. Published by Elsevier Inc. All rights reserved.

very intense radiation. These local hot spots are not important for highly conductive absorbers, but numerous practical systems are required to eliminate them (Tabor, 1984). On the other hand, thermal performance abates due to the heat loss; thereupon, an extensive study has been conducted to evaluate the various routes of heat loss (Hirasawa et al., 2013; Ouagued et al., 2013). Other issues are an additional incurred cost of the sun tracking system and its power consumption, as well as the maintenance of its moving parts.

One alternative for concentrating collectors to abolish the necessity of sun tracking systems are compound parabolic concentrators (CPCs), which are non-imaging concentrators. These devices are relevant for solar energy collection because they achieve the highest possible concentration for any acceptance angle and can utilize direct and diffuse solar radiation (Rabl, 1976a). Thus, a CPC is expected to be more effective than a normal flat plate solar collector in the context of increased heat flux in high temperature applications (Kim et al., 2008). Since the introduction of CPCs, extensive research has been conducted, aiming to analyze their properties and improve the design (Hinterberger and Winston, 1966a, 1966b). Mcintire (1980) had designed a new reflector for the region below a tubular absorber to eliminate the solar radiation loss through gaps between the absorber and reflector. Oommen and Jayaraman (2001) analyzed the performance of a CPC with reduced gap losses and oversized reflector, and the CPC was fabricated for steam generation. Other CPC configurations were proposed, such as CPC with flat bifacial absorber that was proposed by Tripanagnostopoulos et al. (1999) and asymmetric compound parabolic concentrator that was proposed by Adsten et al. (2004). Gudekar et al. (2013) proposed a cost–effective design of CPC for steam generation. The proposed system required much smaller mirror area compared to the conventional CPC design, whereas it required tilt adjustments to be performed after every 6 h of operation.

Another design for non-imaging concentrators are involute collectors. Maruyama (1993) proposed an involute reflector for generation of uniform and homogeneous emission and performed ray-tracing calculation to evaluate optical characteristics of that reflector. An integrated collector storage solar water heater, which consists of involute reflectors, was designed, constructed, and studied to evaluate its performance. The design led to non-uniform heat flux distribution on the absorber (Souliotis and Tripanagnostopoulos, 2008).

A two-stage line axis concentrator in an evacuated glass tube was proposed in order to eliminate the drawbacks of conventional collectors and to utilize the advantages of CPCs and involute reflectors. As a first approximation, the concentrator aperture area is considered as an insolation area. The performance of the concentrator was evaluated and temperature uniformity was analyzed (Ustaoglu et al., 2015a, 2015b). Due to the design characteristics of the concentrator, some ray loss occurs from the out of aperture area, because the intercepting area of the reflector is not equal to the glass cover diameter. In other words, when the entire glass tube is considered as an insolation area of the concentrator, only a fraction of solar rays can pass through the aperture area.

To achieve higher solar ray acceptance, the ratio of the reflector aperture area to the glass cover diameter should be increased. Therefore, a dual form of concentrator was considered to achieve increased utilization of incident solar radiation. Besides improved ray acceptance, this configuration is advantageous for multiple concentrator unit applications due to its comparatively less glazing material requirement. Furthermore, the proposed design facilitates the applicability of U-type absorber tube and eliminates the requirement for the unilateral insolation cap on the vacuum glass tube. The objectives of the present study were to evaluate the dual form of the proposed concentrator with an emphasis on its optical and thermal efficiencies and to analyze the seasonal performance. For the seasonal performance analysis, an evaluation method was adopted by using a 2-D ray tracing model. The design bears a promise to be used in systems of multiple concentrator units; hence, it can be used in high-temperature applications, such as steam generation.

2. Geometry and methods of analysis

2.1. The geometry of a concentrator

The design of the concentrator is mainly based on the exploitation of the uniform distribution of temperature on the absorber and on approaching the highest possible concentration by reflectors. The concentrator is implemented by using an involute reflector with tubular absorber configuration and a compound parabolic reflector. In order to eliminate the convective and conductive heat losses, the configuration is covered by an evacuated glass tube. The schematic of a typical solar concentrator is shown in Fig. 1.

The concentrator is designed by determining the location-dependent acceptance angle of a CPC (Ustaoglu et al., 2015a, 2015b). Because the absorber surface area is equal to the aperture area of the involute reflector, the optimized configuration of reflector and absorber can be derived by using a fixed absorber diameter of 0.01 m. One, however, should keep in mind that all size parameters of the concentrator are proportional one to another and all of them depend on the absorber tube radius. The glass cover size is determined for the least possible radius and it is 0.075 m in the case of a single concentrator. The CPC reflector profile of the proposed concentrator has been designed for the Sendai, Japan, and its half acceptance angle was estimated as 23.44°.

For real applications, the entire area of the concentrator should be treated as solar insolation area. Consequently, some of the incident rays come to naught from the sides of the glass tube, as is shown in Fig. 3. In order to utilize as much solar irradiance as possible, the ratio of the aperture area to the glass cover diameter should be increased. Moreover, the concentrator's height-to-width ratio should be close to 1 to obtain the optimal reflector size for the evaluation of space in the glass tube. In this respect, a dual concentrator is likely to be one of the best candidates because of its proper size. In the case of a dual concentrator, the same amount of energy that is obtained from a single concentrator can be utilized by using smaller insolation area and comparatively less glass material requirement. From a different viewpoint, using three or more combined reflectors substantially increases the manufacturing cost because of the incremental increase of evacuated glass tube price and makes the configuration unwieldy. Thus, a dual concentrator can meet the expectations on concentrator efficiency and cost.

As shown in Fig. 2, the dual concentrator comprises two pieces of solar concentrators. The radius of the glass is 0.0975 m and the circumference is 1.22 m, for the same radius as that of a single concentrator. Although two combined reflectors were used in the dual concentrator, the circumference of the glass cover was slightly increased (by 28%). Therefore, a dual concentrator can provide low material usage for

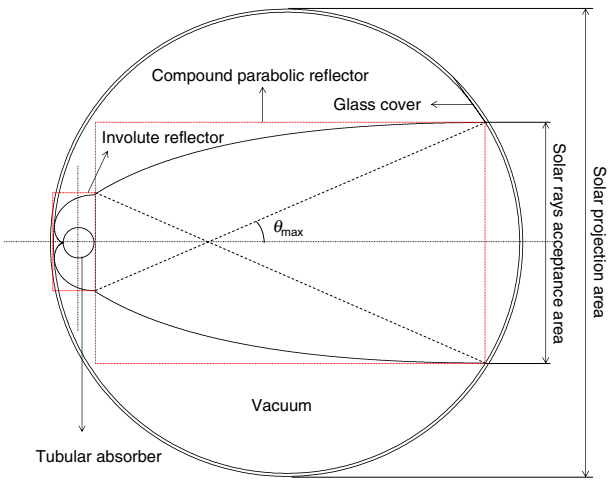

Fig. 1. Geometry of the proposed concentrator.

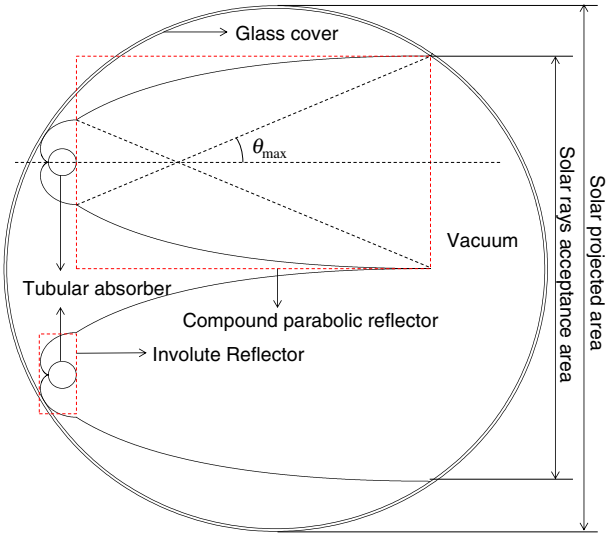

Fig. 2. Geometry of the dual concentrator.

multiple collector applications and pave the way for more proper fabrication of, e.g., U-type absorber tubes.

2.2. Evaluation of optical efficiency

Optical efficiency η_{opt} refers to the amount of the incident solar radiation absorbed by the absorber and it is a function of the absorptivity α_{ab} of absorber, transmissivity τ_c of glass cover, and reflectivity ρ_r of the reflector. To evaluate the optical efficiency as a function of the angle of incidence, a ray tracing model for the 2-D geometry has been developed in FORTRAN. First, incident solar radiation is divided into a number of rays (Nr) and the energy of each ray is set. Thus, ray tracing can give the number of rays captured along with the concentrator's aperture area (n), the amount of energy absorbed by the absorber for different angles of incidence, and the number of times (Rn) each ray is reflected before reaching the absorber. Therefore, the optical efficiency of the concentrator is defined as:

$$\eta_{opt} = \frac{\sum_{i=1}^{i=n} \rho^{Rn}}{Nr} \alpha_{ab} \tau_c \quad (1)$$

A ray is traced numerically according to the following rules. All rays entering the aperture at incidence angles within the half acceptance angle θ_{max} reach the absorber either directly or after several reflections. When a ray hits the glass cover, the ray's intensity is reduced depending on the glass transmissivity, following which the ray continues in the same direction for a glass tube having small enough thickness and curvature. However, it is important to state that incident rays deviate as well as change direction depending on the thickness and curvature of the glass cover. When a ray hits the reflector surface, the ray's intensity is reduced depending on the reflector's reflectivity, following which the reflected ray is traced again. When a ray hits the absorber surface, the ray is wholly absorbed depending on absorptivity and the hit point's position is recorded. When the rays arrive at an incidence angle of 23.44° (the acceptance angle), all rays converge on the focus point of parabola, which is the connection point of parabolic and involute reflectors. Rays that are out of the acceptance angle return back into the ambient. In order to simplify the analysis, the following conditions were assumed:

(1) Absorptivity, transmissivity, and reflectivity are independent of incidence angles.
(2) The concentrators are ideal and free from fabrication errors.
(3) All reflections off the reflector surfaces are specular.
(4) Only direct solar irradiation is accounted for and its angle is varied as the calculation parameter.
(5) Incident solar irradiance is divided into 1000 rays.
(6) The concentrator is discretized into 3500 elements.
(7) The entire glass cover area is considered as a solar projected area on the concentrator that is related to the ray acceptance.

Table 1 shows the optical efficiency calculation parameters for the ray tracing model. The model was validated in the previous study

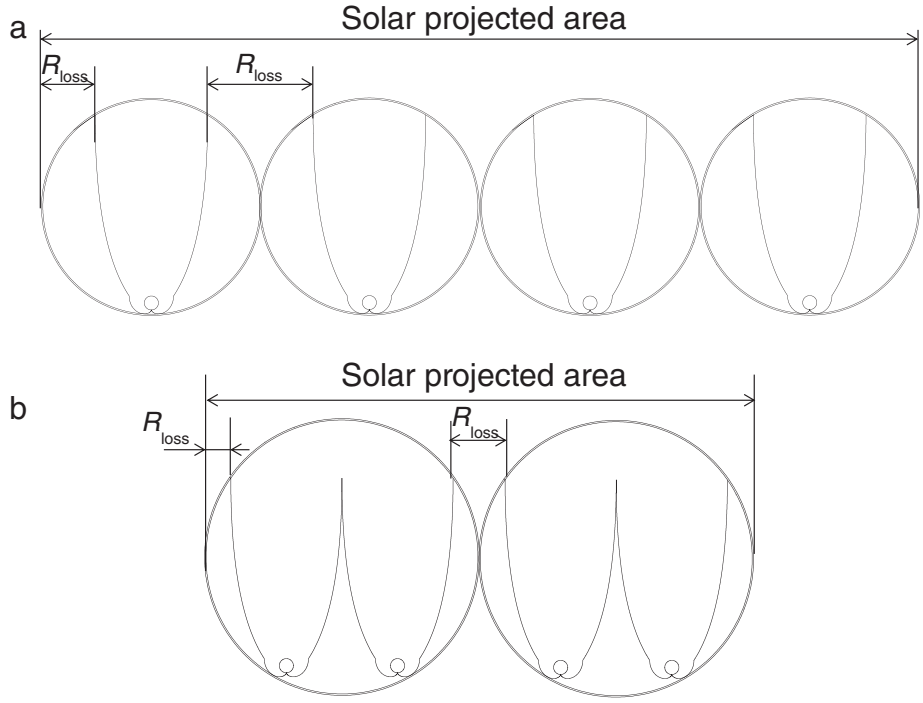

Fig. 3. Applications of (a) single and (b) dual concentrators in multiple reflectors.

Table 1
Specifications of concentrator materials.

Concentrator parameter	Value
Glass tube transmissivity (τ_c)	0.95
Absorber's absorptivity (α_{ab})	0.90
Reflector's reflectivity (ρ_r)	0.90

(Ustaoglu et al., 2015a, 2015b) by comparing our calculation results with those obtained from other CPC studies that were performed by Rabl (1976) and Su et al. (2012). The data for the comparison were taken from a conventional CPC having the same conditions and were sufficiently close to our results (Ustaoglu et al., 2015a, 2015b).

2.3. Evaluation of thermal efficiency

The absorber is covered entirely within the cavity formed by the reflector mirror and glass cover. After being transmitted through the glass cover and reflected from the specular surface, the insolation q_s is absorbed by the receiver pipe based on the absorbing ability. The useful energy gain depends strongly on the energy losses from the absorber, due to both the convective heat loss to the ambient air and radiative heat loss to its surroundings. When both the absorber and the enclosing surfaces are isothermal, radiative exchange factor can be easily modeled. Assumption of the gray body conditions, the net radiation rate transferred from absorber to the enclosing surfaces can be expressed as follows (Snail et al., 1984; Eames and Norton, 1993):

$$q_r = \varepsilon\sigma A_a\left(T_a^4 - T_c^4\right) \tag{2}$$

where σ indicates the Stefan–Boltzmann constant, A_a is the surface area of the absorber, T_a and T_c are the absorber and glass cover temperature, respectively. When the cavity wall temperature is non-uniform, the use of radiative exchange factor or view factor will be necessary for the long-wave radiative exchange. In the case of the proposed design, the uniform solar illumination around the absorber can be achieved due to the design characteristic (Ustaoglu et al., 2015a, 2015b). Moreover, the involute reflector with a cylindrical absorber can provide a uniform isotropic emission from the aperture of the reflector (Maruyama, 1991). Thus, Eq. (2) can be used to calculate the radiative heat loss phenomena from the absorber as a first approximation. On the other hand, the glass cover temperature is close to the ambient temperature rather than the absorber. Therefore, the glass cover temperature can be considered to be ambient temperature in order to facilitate the evaluation.

The convective and conductive heat loss from the absorber can be expressed as follows.

$$q_c = UA_a(T_a - T_{amb}) \tag{3}$$

where U is the overall heat transfer coefficient in terms of convective and conductive heat losses. T_{amb} is the ambient temperature.

In this case, the useful energy can be expressed as (Howell et al., 1982):

$$\dot{Q}_u(t) = q_u(t)A_c = \eta_{opt}q_s(t)A_c - UA_a(T_a - T_{amb}) - \varepsilon\sigma A_a\left(T_a^4 - T_{amb}^4\right) \tag{4}$$

In Eq. (4), the optical efficiency η_{opt} accounts for the effects of transmission, reflection, and absorption losses due to the cover glass, reflectors and absorber, or other optical losses in the concentrator. The term $q_s(t)\ A_c$ refers to an instantaneous solar insolation per unit aperture area of the concentrator. Therefore, the first term indicates the energy absorbed by the concentrator's absorber.

The second term describes the convective and conductive heat losses in terms of overall heat transfer coefficient U from the absorber area A_a between the average absorber temperature T_a and ambient temperature T_{amb}. The final term describes the radiative heat loss from the absorber to its surroundings, depending on the emissivity ε of the absorber. The sky temperature is assumed same as the ambient temperature. Thus, the concentrator efficiency, which is the ratio of the useful energy to available energy, can be obtained as follows:

$$\eta_{th} = \frac{\dot{Q}_u(t)_c}{q_s(t)A_c} = \eta_{opt} - \frac{UA_a(T_a - T_{amb})}{q_s(t)A_c} - \frac{\varepsilon\sigma A_a\left(T_a^4 - T_{amb}^4\right)}{q_s(t)A_c} \tag{5}$$

The ratio of the concentrator aperture area to absorber area, or the aperture area of the involute reflector, describes the concentration ratio C as given by Eq. (6):

$$C = \frac{A_c}{A_a} = \frac{1}{\sin\theta_{\max}} \tag{6}$$

Rearranging Eq. (5) by eliminating the conductive and convective heat losses due to the evacuated glass cover, one obtains Eq. (7):

$$\eta_{th} = \eta_{opt} - \frac{\varepsilon\sigma\left(T_a^4 - T_{amb}^4\right)}{q_s C} \tag{7}$$

Since only direct solar irradiation was taken into account, the solar heat flux q_s can be determined from the following equation:

$$q_s = I_{in}\cos\theta \tag{8}$$

where θ is the incidence angle and I_{in} is the solar beam intensity. In order to calculate the concentrators' thermal efficiency, some general assumptions were made such as the uniformity of temperature throughout the surface of each reflector, and the absorptivity, transmissivity, and reflectivity were considered independent of the angle of incidence. The effect of the glass cover in the radiative heat loss phenomenon was neglected. However, it is important to state that although the glass cover is assumed transparent for visible light and nearly opaque for the thermal radiation in the infrared region, the thermal properties of the glass cover including transmissivity, reflectivity and absorptivity depends on the function of wavelength, incidence angle of the solar radiations and the real and imaginary part of the complex refractive index of the glass cover (Khoukhi and Maruyama, 2005). Thus, the effective value of the emissivity of the absorber is affected from the glass cover and the glass cover reduces the radiative heat loss as well as convective heat loss. In order to facilitate the evaluation and as first approximation, this effect was not taken into account in this study. Thermal emissions from the reflector and the ambient were neglected. The solar beam intensity I_{in} was assumed as 1000 W/m^2. The solar insolation changes while incident angle varies as seen in Eq. (8). The absorber was considered for gray and selective surface cases. Thermal emissivity ε of selective coated absorbers in the infrared region was assumed as 0.07 and the emissivity was considered to be 0.9 for a gray surface absorber. Absorber temperature T_a was assumed to be uniform throughout the receiver tube and its value was fixed at 373 K and ambient temperature T_{amb} was 293 K. Temperature distributions on the absorber were evaluated to validate the uniformity assumptions that were made in the previous study for different absorber materials such as copper, aluminum and stainless steel (Ustaoglu et al., 2015a, 2015b). The results suggest that the assumption of temperature uniformity on the absorber was reasonable. The calculation was conducted for Sendai, Japan.

2.4. Evaluation of seasonal efficiency

The proposed concentrator is oriented with its line axis along the East–West direction, and its aperture is tilted southward, as shown in Fig. 4. The acceptance angle $\theta_{\max}$ was determined for year-around utilization of solar radiation, between winter and summer solstice. Solar altitudes α_s (Eq. (9)) were calculated as follows at the solar noon for the

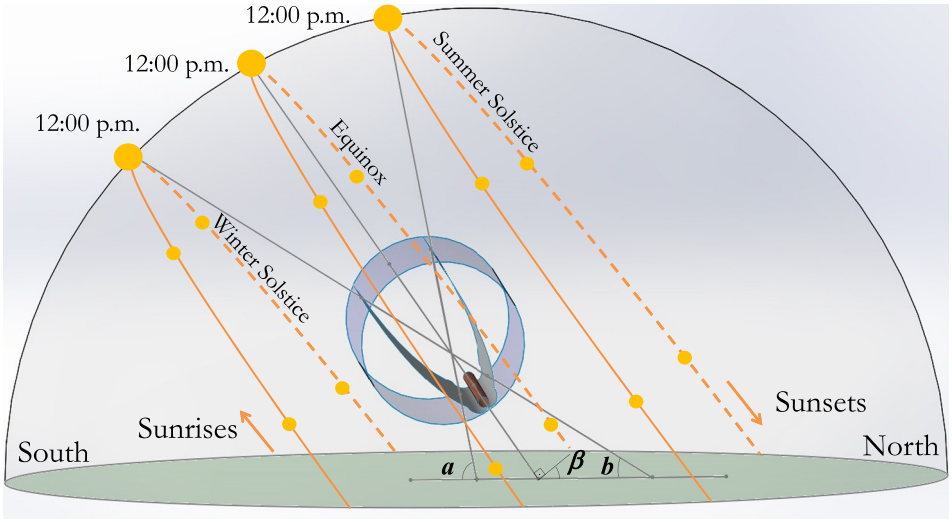

Fig. 4. Position of the proposed solar concentrator with respect to the solar altitude.

winter solstice, December 21 and the summer solstice, June 21, and were 75.19° and 28.3° respectively, for Sendai, Japan:

$$\sin\alpha_s = \sin\phi\sin\delta + \cos\phi\cos\delta\cos\omega \tag{9}$$

where ϕ is the latitude, Ω is the hour angle, and δ is the declination. Using the solar altitude angles a and b (for summer and winter solstice, respectively), θ_{max} and tilt angle β can be determined from $\theta_{max} = (a - b)/2$ and $\beta = (\pi/2) - (a - \theta_{max})$. Hence, the calculated half-maximum acceptance angle and the tilt angle were 23.44° and 38.25°, respectively. In this case, the concentrator can achieve the concentration ratio of 2.51.

During a day or during seasonal variation, some rays reach the concentrator's reflectors at oblique angles, as shown in Fig. 4. Therefore, in order to determine the seasonal performance, the concentrator should be considered in three-dimensional space. The direct solar irradiance can be considered as a vector with two orthogonal components in North–South and East–West vertical surfaces. When the concentrator is oriented with its long axis along the East–West direction, only the projection of direct irradiance component on the North–South vertical surface can be considered, since East–West component is parallel to the absorber pipe and does not contribute energy flow on the absorber surface but shadows the effect due to the vacuum tube cap.

As a first approximation, a specular reflection of the incoming light is considered. An incident ray, marked I, from a light source is striking the reflector's surface at an incidence angle θ_{3D}. This ray, marked R, is reflected from the reflective surface at the same angle and hits an object at point C, as is shown in Fig. 5a. The projection of the incident ray I and reflected ray R on the 2D surface front view becomes I_p and R_p, respectively, as in Fig. 5b, while the angle of incidence θ_{3D} changes to θ_{2D}. If the incidence angle θ_{2D} can be defined, the direction of the reflected ray and the position of the hit point on 2D surface can be obtained by using a 2D ray tracing method.

In the case of the proposed concentrator, the projection of an oblique incident ray in 3D space is shown in Fig. 6. Here, the direction of the reflected ray and its hit point of the absorber on 2D surface can be defined. If the absorber of the line-axis concentrator is assumed long enough to eliminate end ray loss from the front and back sides of the concentrator, the performance can be evaluated for any oblique angle of incidence by employing the 2D ray tracing method, thereby simulating the seasonal performance.

In order to obtain the equation for θ_{2D}, a direct ray arriving at an incidence angle θ_{3D} is considered, as shown in Fig. 7, and its projection angle in North–South 2D plane is θ_{2D}. The angle between the surface normal N and the concentrator normal N_{con} indicates the location's latitude. Since the concentrator is oriented with a tilt angle β of 38.25°, which is equal to the latitude ϕ of Sendai, the incidence angle θ_{3D} is a normal angle at 12:00 during the equinox day. Using the rule of cosines, the geometric equality of θ_{3D} and θ_{2D} is given by the following equations:

$$(c-x)^2 = \left(b^2 + c^2\right) + \left(x^2 + b^2\right) - 2.\sqrt{\left(x^2 + b^2\right)\left(b^2 + c^2\right)}\cos\theta_{2D} \tag{10}$$

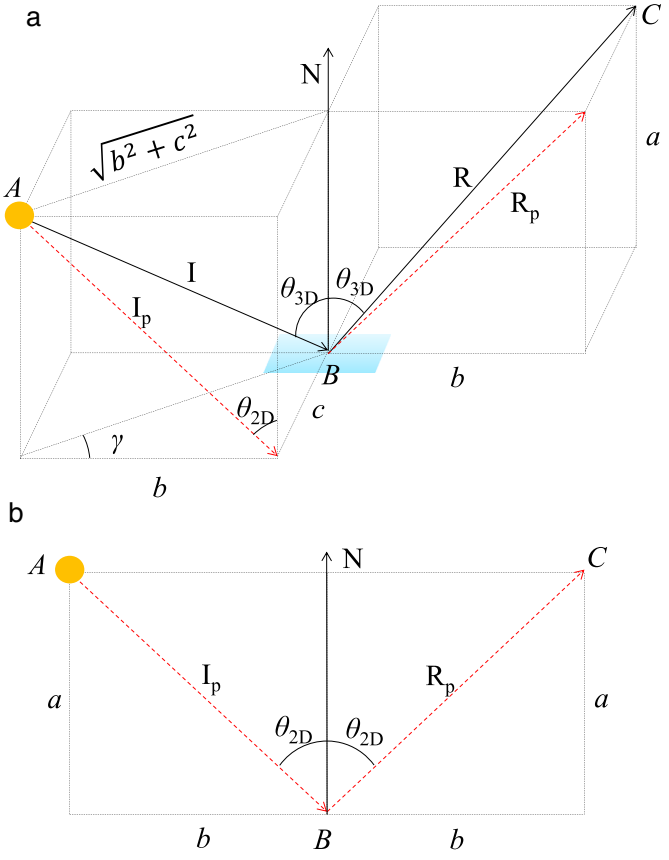

Fig. 5. Reflection of an incident ray in 3D (a) and (b) its front view projection.

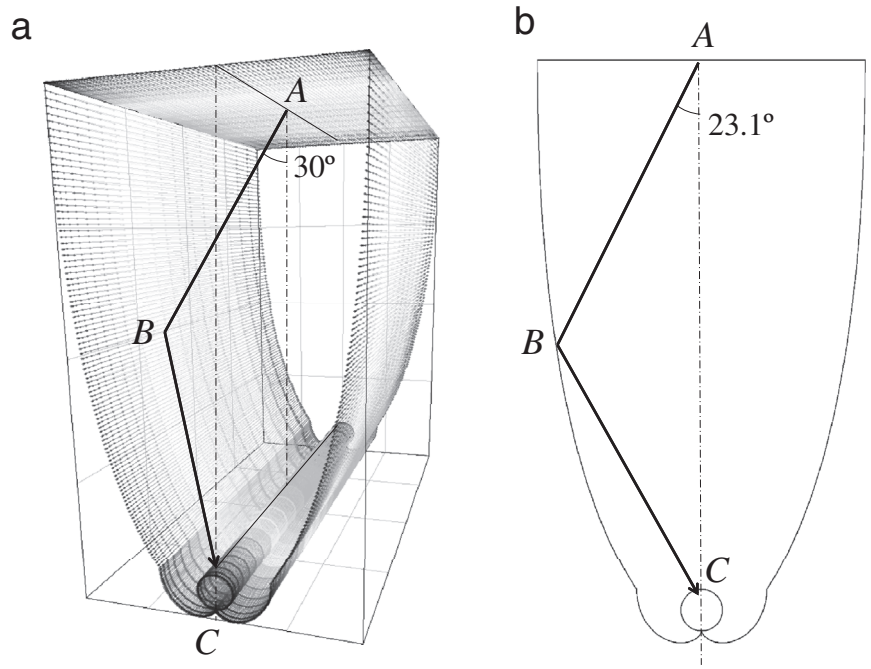

Fig. 6. Reflection of an incident ray in 3D (*a*) and 2D (*b*) geometries. (Sendai, $\phi = 38.25°$, March 20, equinox day at 10:00 a.m., $\gamma_s = 42.41°$, $\theta_{3D} = 30°$, $\theta_{2D} = 23.1°$).

$$a^2 + (c-x)^2 = \left(a^2 + b^2 + c^2\right) + \left(x^2 + b^2\right) - 2.\sqrt{\left(x^2 + b^2\right)\left(b^2 + c^2\right)}\cos\theta_{3D} \tag{11}$$

Solving these equations in conjunction with the geometric equalities of solar altitude α_s and azimuth angles γ_s, the following equation can be obtained:

$$\cos\theta_{2D} = \frac{\cos\theta_{3D}}{\cos\alpha_s\sqrt{\tan^2\alpha_s + \cos^2\gamma_s}} \tag{12}$$

The incidence angle θ_{3D} can be calculated for the concentrator facing the equator as follows, for which the surface azimuth is $\gamma_c = 0$:

$$\begin{aligned}\cos\theta_{3D} &= \cos\gamma_s\cos\alpha_s\sin\beta + \sin\delta\cos\beta \\ &= \sin(\phi-\beta)\sin\delta + \cos(\phi-\beta)\cos\delta\cos\omega\end{aligned} \tag{13}$$

Eventually, rearranging Eqs. (12) and (13), the following equation can be obtained:

$$\cos\theta_{2D} = \frac{\cos\gamma_s\cos\alpha_s\sin\beta + \sin\delta\cos\beta}{\cos\alpha_s\sqrt{\tan^2\alpha_s + \cos^2\gamma_s}} \tag{14}$$

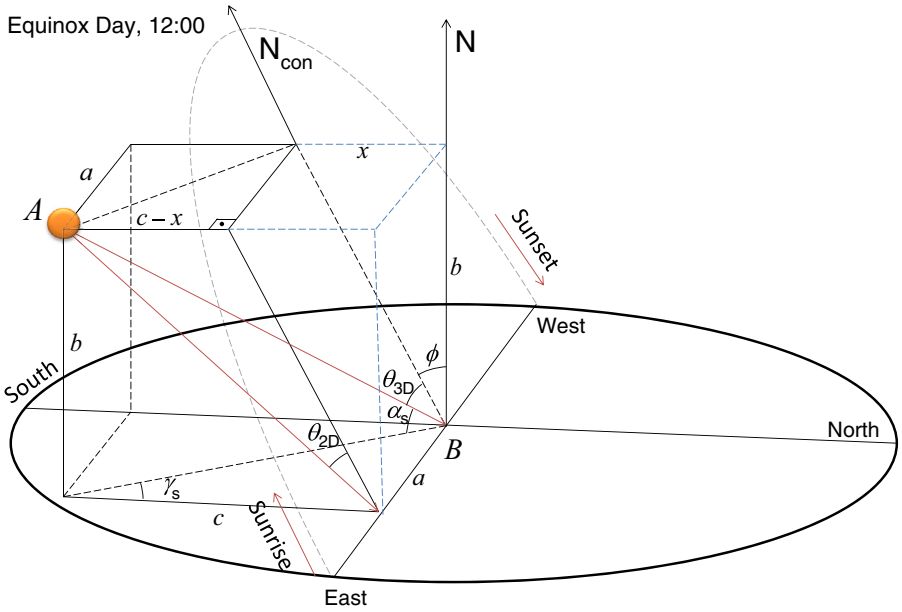

Fig. 7. Position of the sun with respect to the concentrator normal.

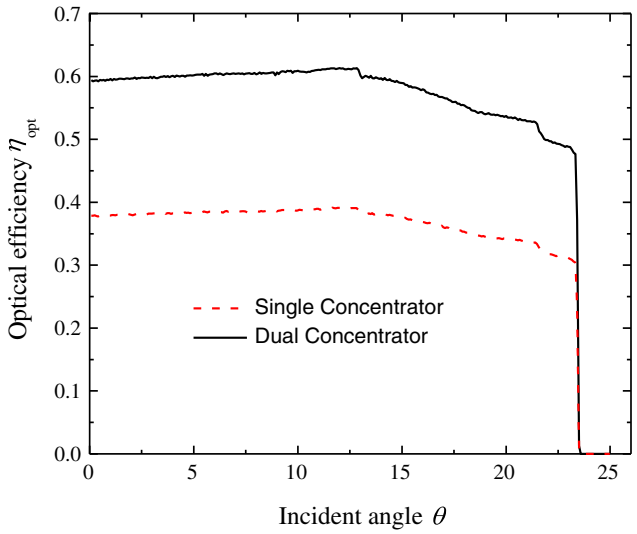

Fig. 8. Optical efficiency vs. the angle of incidence.

Solar azimuth angle γ_s can be described in terms of δ, Ω, and α_s as follows:

$$\sin \gamma_s = \frac{\cos \delta \sin \omega}{\cos \alpha_s} \tag{15}$$

In order to determine the direction of reflected rays and hit points of incident rays, the incidence angle θ_{2D} on 2D surface is essential, while determination of the incident solar irradiation's heat flux requires the incidence angle θ_{3D} ($q_s = I_{in} \cos \theta_{3D}$). Thus, seasonal performance can be estimated approximately. This method can be applied to any line-axis solar concentrator system. The incidence angle's projection was evaluated by some authors (McIntire and Reed, 1983; Pinazo et al., 1992).

3. Results and discussion

3.1. Optical efficiency

The optical efficiency is related to the process in which a spectral component of incident solar radiation is transmitted through the evacuated glass cover, reflected secularly from the reflector's surface and absorbed by the tubular absorber. A brief examination of Eq. (1) reveals that, while the concentration ratio of the concentrator tends to infinity, η_{opt} tends to its minimum due to an increased number of reflections. Hence, an optimal size and a higher value of the optical parameters with optimal cost are likely to improve the performance significantly.

In the 2D calculations of optical performance, all concentrator specifications that were considered are given in Table 1. The concentrator sizes were determined for the absorber's external diameter of 20 mm. The considered time was 12:00 p.m. for incidence angles within the acceptance angle of 23.44°. All rays entering the concentrator aperture within the acceptance angle θ_{max} reach the absorber either directly or after several reflections, and all rays with angle of incidence beyond θ_{max} are rejected.

As a first evaluation, the case of the normal incidence angle was considered for both concentrators. Only 52% of rays can enter the aperture of the single concentrator, and as many as 82% of rays can enter the aperture of the dual concentrator. This is likely to yield higher optical efficiency for the dual concentrator as compared to the single concentrator. The ray loss from the sides of the concentrator is likely to increase as the angle of incidence approaches the acceptance angle.

Fig. 8 illustrates the dependence of optical efficiency on the incidence angle θ for the dual and single concentrators, under the condition of spectral solar radiation. The performance of the single concentrator is more stable as compared to that of the dual one. As the angle of incidence approaches 12°, the performance of both concentrators increases slightly. In the case of dual concentrator a maximal efficiency of 61.3% is obtained for the angle 12° at which the efficiency of the single concentrator is 39.16%. For angles of incidence higher than 12° performance decreases gradually and a stronger reduction of performance is observed around 21.4°. Furthermore, when the angle of rays' incidence reaches the acceptance angle, the number of reflections increases, thereby resulting in a sharp drop in the optical efficiency. Additionally, in accordance with the angular alternation of ray acceptance, the efficiency of the dual concentrator decreases more compared to that of the single one. In other words, the difference between the maximal and minimal optical efficiencies is about 15% for the dual case, and that of the single one decreases by 9.3%. The average optical efficiency of the dual concentrator is about 57%, and that of the single one is 37%.

It is important to state why the concentrator shows the maximum performance in the case of the incident angle of 12°. Fig. 9 illustrates the ray tracing on the dual concentrator for the normal incident angle, the incident angle of 12° and the incident angle of 23°. In the case of the normal incident angle, a tiny fraction of the solar radiation pass through the aperture area of the concentrator can reach to absorber directly, and the major part hit the reflector first. The rays hit the upper part of the CPC reflector may reflect more than one time on the CPC reflector surface (Rabl, 1976b). After first or second reflection from CPC, some rays reach to the involute reflector while some of them reach to

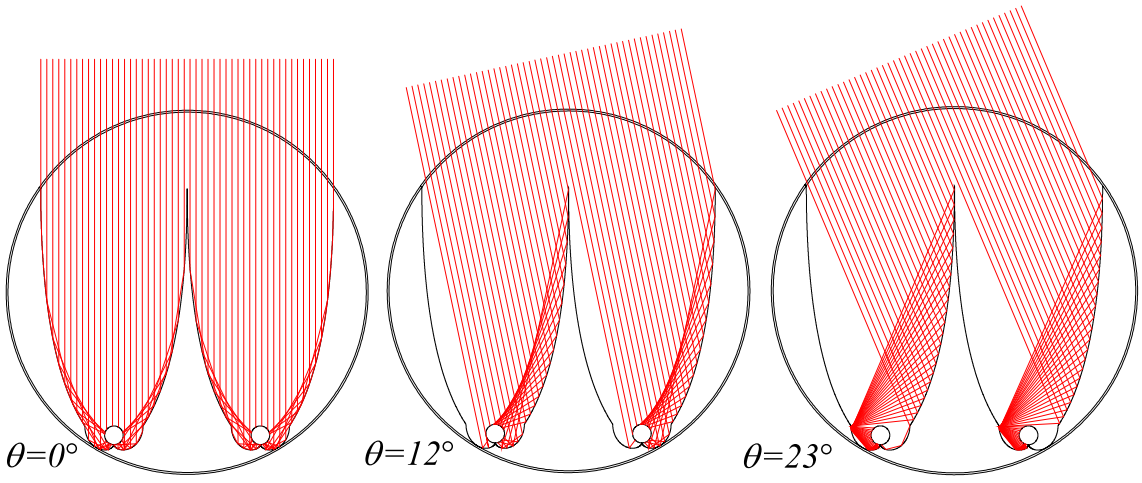

Fig. 9. The ray tracing on the dual concentrator for the normal incident angle, incident angle of 12° and 23°.

the absorber. As is known, the optical performance decreases depending of the number of reflection of rays in accordance with the reflectivity. As the incident angle of the rays approach to 12°, most of the rays reach to the absorber after only one reflection from the CPC. On the other hand, for the maximum incident angle case, almost all rays reach to the upper part of the involute reflector after one reflection on CPC and the major part of those rays reflect for second times in the involute reflector. Thus, the optical performance decreases significantly. In the same way, as the incident angle of the rays approach to 12°, the number of rays hit the absorber after only one reflection increases. Therefore, the maximum performance was achieved around the incident angle of 12°.

3.2. Thermal efficiency

Thermal efficiency is a function of optical efficiency and heat losses from the absorber. Heat loss can be mediated by convective, conductive, or radiative heat transfer mechanisms. Because heat transfer by convection and conduction requires transfer media, the associated heat losses do not exist in vacuum. Evacuated glass tube also protects the reflector's surface from external conditions and the absorber from wind effect that is likely to increase the heat loss. In radiative heat loss calculations, the surrounding temperature was assumed to be 293 K. The evaluations were conducted for that efficiency as a function of the angle of incidence and absorber temperature. The concentration ratio was set as 2.51 for both concentrators. The incident solar irradiance was assumed to be 1000 W/m^2 and its intensity depends on the angle of incidence. The working fluid temperature in the absorber's outlet depends on the mass flow rate. However, in the present calculation, absorber's temperature was evaluated as a calculation parameter by using Eq. (7).

Recently, selective coating absorbers have found widespread use in connection with lower thermal emissivity effect. The concentrator's performance can be substantially increased by reducing the radiative heat loss from the absorber. Therefore, the effect of spectral selective coating on the performance of the proposed solar concentrators was considered as well, in addition to the effect of gray surface. The efficiency was calculated for a selective coated surface with thermal emissivity ε of 0.07.

The effect of gray surface and selective coating on the concentrator's thermal performance is shown in Fig. 10 for different angles of incidence and absorber temperature of 373 K. While the angle of incidence varies between the angle of normal incidence and the acceptance angle, the time represented is 12:00 p.m., as noted in Fig. 4.

First, because of its higher ray acceptance, a dual concentrator operates with higher efficiency than a single concentrator, for both gray surface and selective coating cases. Regarding the smaller number of reflections, maximal efficiencies are obtained for the incidence angle of about 12°. As a general rule, while the angle of incidence increases, the intensity of the incident solar irradiation wanes (Eq. (8)). It is expected that, as the angle of incidence approaches the acceptance angle, the performance will decrease with regard to the decreasing heat flux. Contrary to this expectation, the reduction of the performance is observed merely after the maximal efficiency angle of 12°. The effect of heat flux reduction on performance becomes more evident in the case of a gray surface as compared to the selective coating case, because selective surface can reduce its potency on performance with decreasing radiative heat loss.

In the case of dual concentrator with gray surface absorber, an average thermal efficiency of 33.63% is obtained, while a single concentrator exhibits average thermal efficiency of only 12.6%. The efficiency of the single concentrator is increased owing to the effect of selective surface, and approaches the efficiency of the dual concentrator with gray surface. The average efficiency of a dual concentrator with selective coating absorber can reach 56%, while that of a single concentrator reaches 35%. Furthermore, the maximal thermal efficiency of a dual concentrator can reach 59.5% while a single concentrator has the maximal thermal efficiency of 37%. Spectral selective coating significantly enhances performance.

Fig. 11 shows thermal efficiencies of dual and single concentrators as a function of absorber temperature, for selective coating and gray surface absorbers. The angle of incidence is considered to be normal. Absorber's temperature is varied as a calculation parameter. Heat loss from the absorber does not exist when the absorber temperature is equal to the ambient temperature. Therefore, at this temperature, the efficiency is equivalent to the optical efficiency. As the temperature difference grows, thermal efficiency decreases up to a maximal absorber temperature.

A gray surface absorber is not suitable for high temperature applications such as steam generation because of the high thermal loss. In other words, a sharp reduction of performance along with the increase of absorber's temperature prevents from obtaining high absorber temperature and performing with optimal efficiency. Selective coated absorbers are essential for heat and steam generation. Thus, a dual concentrator operates with thermal efficiency of 52.7%, while a single one can reach the efficiency of 31% even for absorber temperatures as high as 473 K.

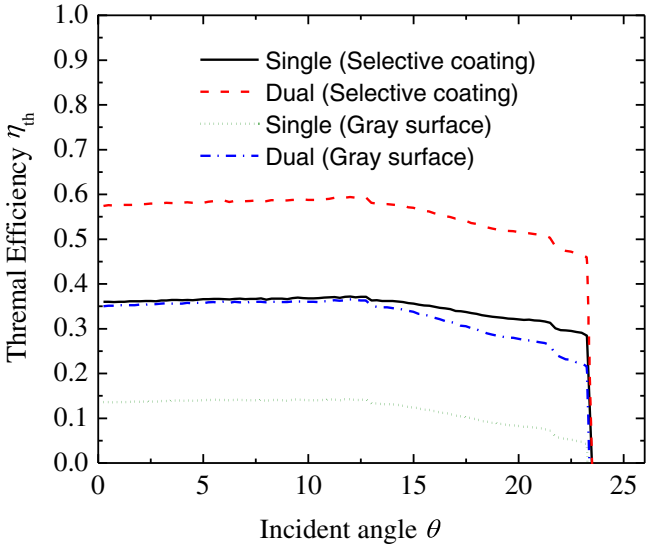

Fig. 10. Thermal efficiency as a function of incidence angle, for different scenarios of absorber surface.

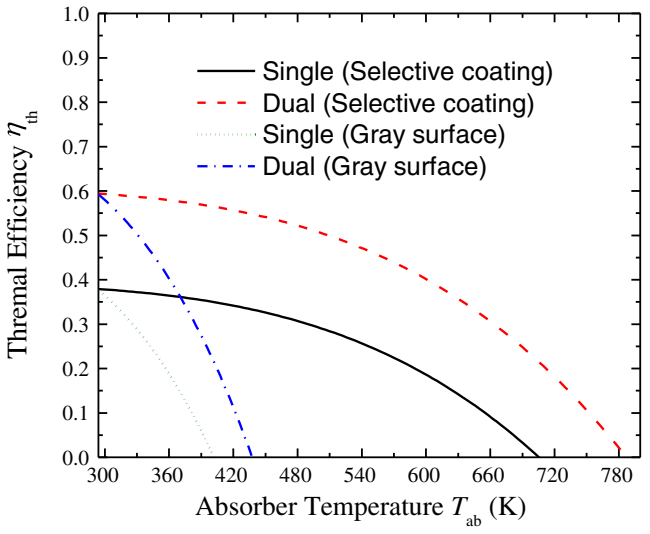

Fig. 11. Thermal efficiency as a function of absorber temperature, for different scenarios of absorber surface.

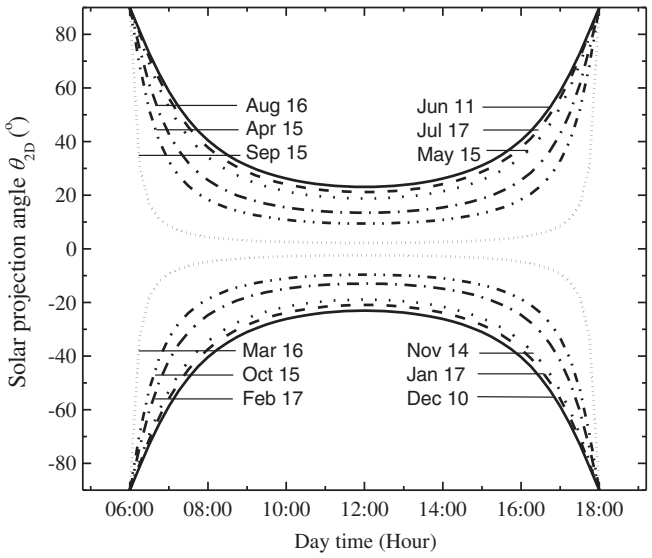

Fig. 12. The solar projection angle on 2D surface, as a function of time during the day.

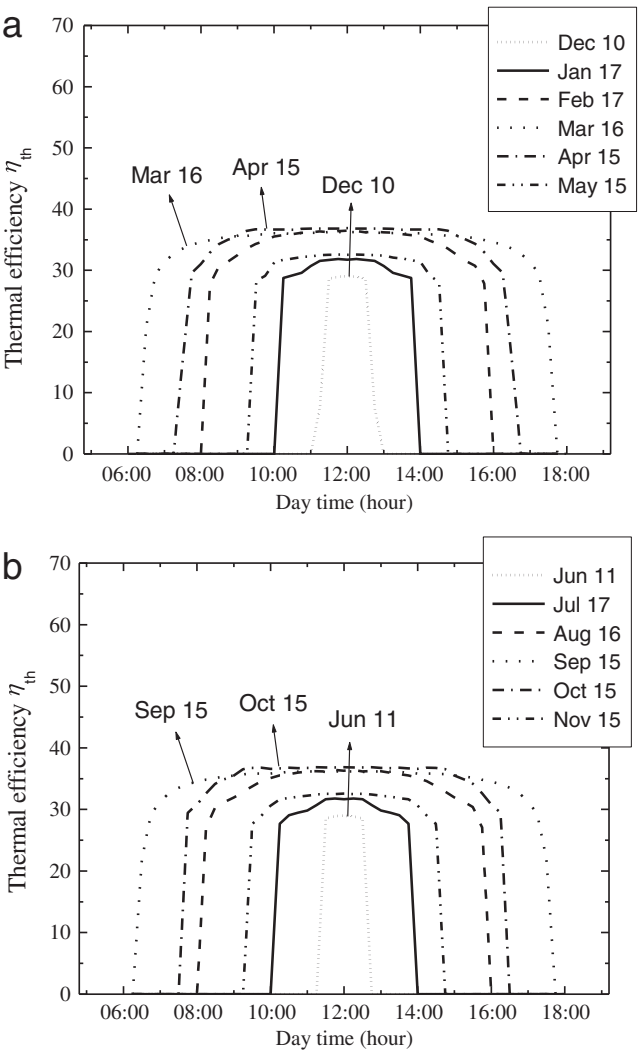

Fig. 13. Thermal performance of single concentrator as a function of time during the day.

3.3. Seasonal performance

Another comparison was conducted to evaluate the seasonal performance. The orientation and design parameters of the concentrator are discussed in detail in the section that describes the calculation method.

Fig. 12 illustrates the solar projection angle for the proposed concentrator during different days and hours. The days are 17th (Jan 17), 47th (Feb 16), 75th (Mar 16), 105th (Apr 15), 135th (May 15), 162th (Jun 11), 198th (Jul 17), 228th (Aug 16), 258th (Sep 15), 288th (Oct 15), 318th (Nov 14), and 344th (Dec 10) days of a year and the corresponding characteristic days of each month. The negative value of the incidence angle indicates that the sun is between the winter solstice and equinox day. The values of θ_{2D} on March 16 and September 15 are stable during the day and are very close to the angle of normal incidence, because these days are close to the equinox days. As the sun approaches the winter and summer solstice days, the angles of incidence approach the acceptance angle. Accordingly, the concentrator can utilize the solar irradiation mostly for the angles of incidence that are close to the angle of normal incidence.

The angle θ_{2D} is symmetric with respect to the equinox and solstice days. Therefore, thermal performance of the single concentrator is evaluated only for half of the year on selected days. The optical properties of the concentrator are assumed to be as in Table 1. The absorber is assumed to be coated by the selective surface with thermal emissivity of 0.07. The ambient and absorber temperatures are assumed to be 293 K and 373 K, respectively. The solar beam intensity I_{in} was assumed as 1000 W/m^2 as the solar insolation changes with the incident angle variation depending on the time and location. In this calculation, the effect of the angle of incidence on performance in North–South 2D vertical plane is evaluated to observe the day characteristics with the sun movement. The performance is analyzed for every 15 min, from 6:00 to 18:00.

The concentrator exhibits quite similar performance curves for Dec 10 and Jun 11 and through half of the year, until May 15 and Nov. 15, respectively, as shown in Fig. 13. Thereupon, the comparisons of single and dual concentrators performance as a function of time were conducted for the shortest solar utilization day (SSD) at which the lowest efficiency and shortest solar utilization was obtained, the longest solar utilization day (LSD), and the highest efficiency day (HED), as shown in Fig. 14. To demonstrate the relevancy between these similar days, their solar altitudes α_s are illustrated. On the other hand, due to the similar incidence angle characteristics of the SSD days (Dec 10–Jun 11), LSD days (Mar 16–Sep15), and HED days (Apr 15–Oct. 15), the performances of just Dec 10, Mar 16, and Apr 15 are considered.

In Fig. 14, the axis on the right side corresponds to the angle of incidence θ_{3D}, the projection angle θ_{2D}, and the solar altitude angles α_s. In order to determine θ_{2D}, it is necessary to evaluate the angles α_s and θ_{3D}. The angles α_s on Dec 10 and Jun 11 reach 28.7° and 74.83° at noon, and these values are considerably close to the winter and summer solstice values, while the angles α_s on Mar 16 and Sep 15 are close to each other and to those of the equinox day, and take on the values of 49.33° and 53.96°, respectively. On the HED days, Apr 15 and Oct 15, the solar altitude values are 61.16° and 42.15°, respectively. These values clearly show the characteristics of the sun trajectory on the selected days. The angle θ_{3D} becomes the same as θ_{2D} at noon, and the difference between these two angles becomes larger toward the morning and evening, and then converge again at 6:00 and 18:00.

During SSD, either concentrator can utilize the sun's radiation for a short time. This similarity in the performance of dual and single concentrators indicates that the utilization time is strongly related to the acceptance angle. The angle θ_{2D} decreases until 12:00 and approaches the minimal value of 23°. The concentrator can generate the heat for 2 h, because the angles of incidence are beyond the acceptance angle before 11:00 and after 13:00. The thermal performance of a single concentrator reaches the maximal value of 29% at noon due to the highest solar heat flux, while that of a dual one can achieve the thermal performance of

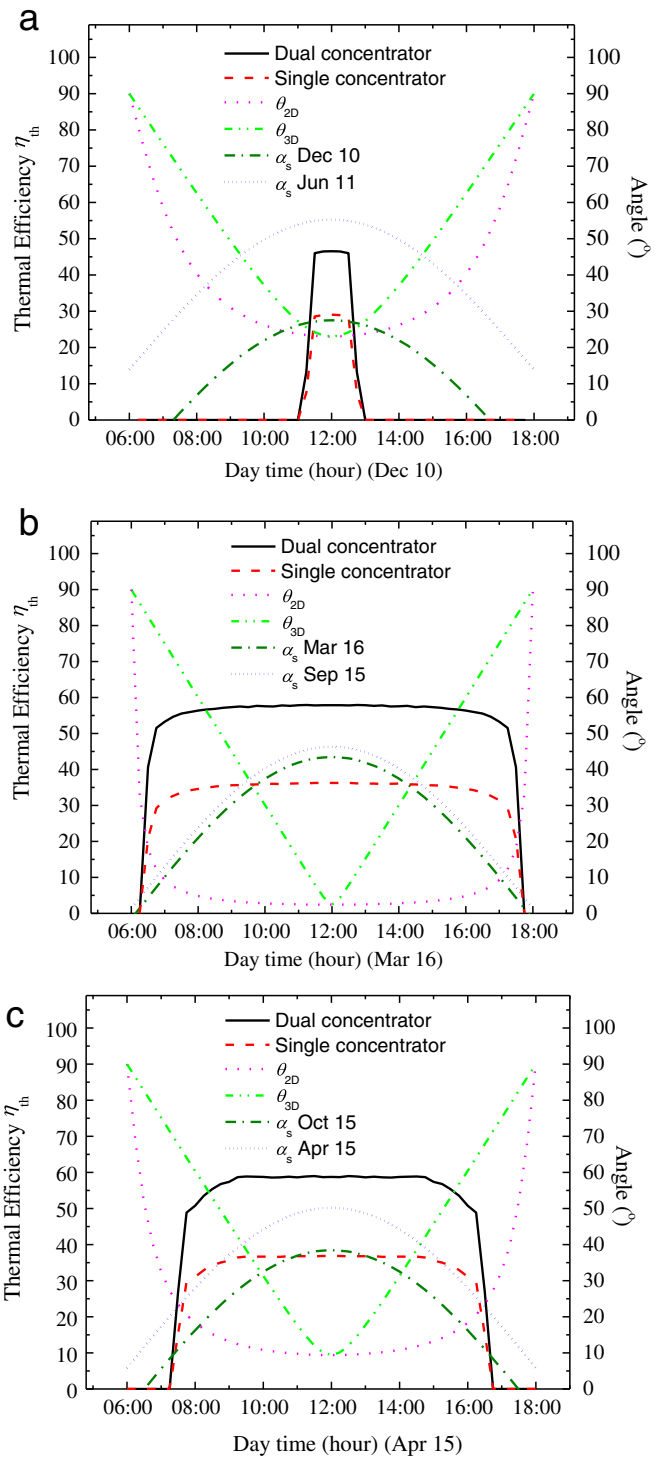

Fig. 14. Hourly thermal efficiency for lowest efficiency and shortest solar utilization day (SSD)(*a*), longest solar utilization day (LSD) (*b*) and highest efficiency day (HED) (*c*).

46.53%. The performances remain stable during the solar utilization time due to the slight variation of solar projection angle. On the other hand, both single and dual concentrators can generate the heat for a long time during the LSD. The angle θ_{2D} remains fairly stable for about 10 h and becomes 2.41° at 12:00. The angle θ_{2D} remains within θ_{max} and near the angle of normal incidence almost for the entire day period. At noon, a single concentrator can reach thermal efficiency of 36.24% while a dual one can achieve the efficiency of 57.9%. The concentrators can utilize solar energy for more than 11 h.

The highest performance is obtained during HED. This slight increase in performance is due to the angle of incidence. The solar projection angle becomes 9.4° at noon, while the average angle is about 13° within the acceptance angle. These angles are quite close to the maximal efficiency angle of 12°; hereby, an improved performance is observed. The solar utilization time reaches 8 h. The thermal efficiency of a single concentrator is 36.9% while that of a dual one reaches 58.8%.

Generally, the highest performance is observed at 12:00, resulting from higher solar heat flux as the efficiency slightly increases for the angle of incidence that is close to the maximal efficiency angle. In addition, the difference in the operating time is irrelevant judging by the day-time characteristic while the key element determining the performance is the value of the solar projection angle. Accordingly, because June 11 is close to the summer solstice day (the longest day), the operation time, and the performance on that day are similar to those obtained for Dec 10 (which is close to the year's shortest day). As a consequence of limited insolation time on these days, little seasonal adjustment is required. Average daily insulation time for 1 year is calculated to be 6 h/day for both concentrators.

The evaluation of concentrators' annual performance was performed to observe the effect of the angle of incidence as a function of time, as shown in Fig. 15. In order to facilitate the evaluation, several assumptions were done. The ambient temperature during the days, the absorber's temperature, and solar intensity were assumed to be constant and were 273 K, 373 K, and 1000 W/m^2, respectively. In order to calculate the solar insolation q_s on the surface of the concentrator, the incident angle of the solar rays was taken into account for each day at 12:00.

The solar projection angle varies between acceptance angles on two different sides of a concentrator and remains within θ_{max} throughout the year. The highest efficiency achieved by the concentrators was 59.36% and 37.2% for dual and single concentrators, respectively, when the angle of incidence was close to the maximal efficiency angle. However, the thermal performances decreased significantly at the end of June and at the end of the year, during which the angle of incidence approached the acceptance angle. Thus, the average efficiencies decreased to 52% and 33% for dual and single concentrators, respectively. Therefore, a slight increase of the concentrator's acceptance angle or a little seasonal adjustment of the orientation can improve the performance for 12:00.

3.4. The proposed collector system with dual concentrator

The proposed concentrator can utilize the advantages of compound parabolic and involute reflectors with tubular absorber design. It achieves highest possible concentration for any acceptance angle and

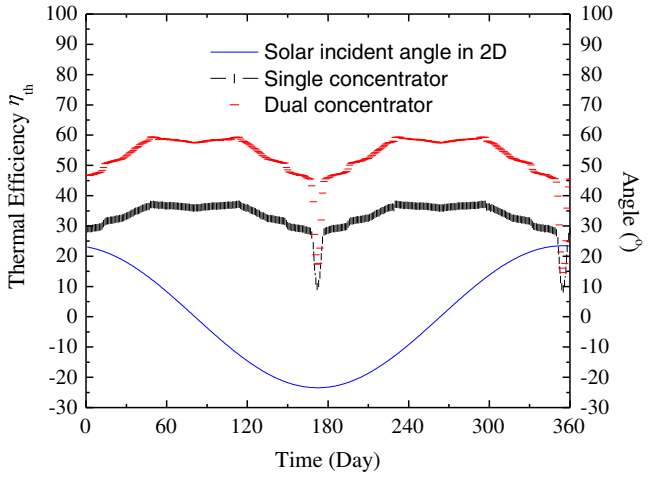

Fig. 15. Annual performance of the concentrators and solar projection angle.

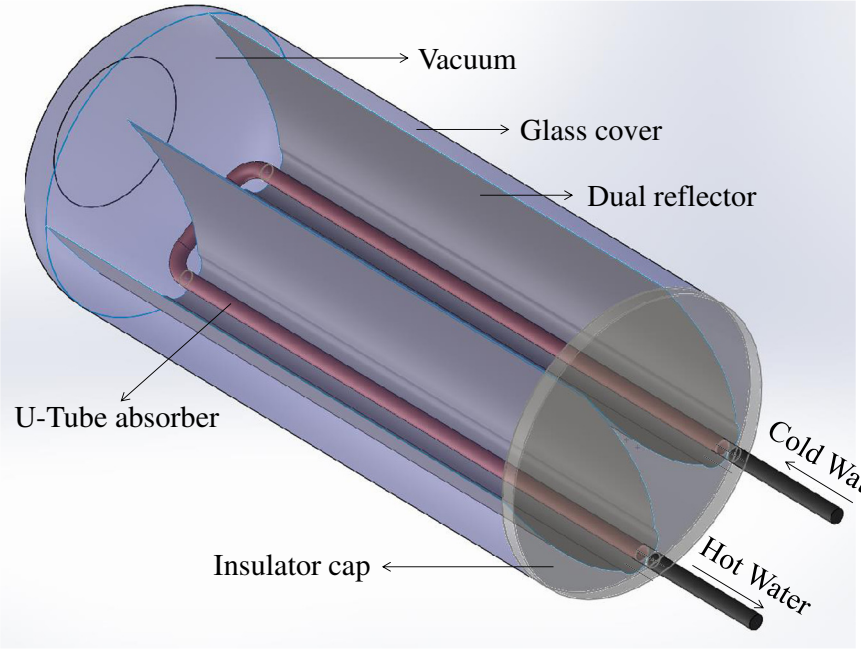

Fig. 16. Top view of U-type absorber pipe in the dual concentrator.

utilizes the direct and diffuse radiation. A uniform temperature distribution can be obtained on the absorber and back side heat loss can be eliminated due to the geometry of the involute reflector with tubular absorber. The convective and conductive heat losses can be eliminated on account of the evacuated glass cover and can also help protect the reflector's surface from external conditions and provide easy maintenance.

Regarding the non-tracking systems, most commonly used collectors are flat plate and evacuated tube collectors. They are usually preferable due to low manufacturing cost. Conventional flat plate collectors are usually suitable for low-temperature applications and their performance is immediately decreased as the absorber temperature is increased. On the other hand, the performance of conventional evacuated tube collector is hereby improved by using selective coating absorber and vacuum tube; this device can be used in higher temperature applications. However, these collectors have the concentration ratio of 1. Therefore, a concentrator system can procure advantages by increasing the heat flux, thereby obtaining higher absorber temperature. The heat loss in the proposed concentrator is minimized and eliminated using selective coating and evacuated glass tube. However, using the evacuated glass tube in a concentrator system may significantly increase the price of the system. Keeping in mind that the cost of a glass tube increases exponentially with the tube radius, it becomes very important to determine the optimal size of the concentrator. One possible approach for cost-effective design is to determine the glass tube's radius according to the common tube size on the market. Hereby, a concentrator collector unit can be constituted to generate a large quantity of high temperature steam by using a sufficiently small tube.

Another cost factor may be the use of selective coating. Although the proposed concentrator with gray surface absorber can produce enough heat for hot water, as a steam generation system, a spectral selective coated absorber is essential to improve the thermal performance due to its reduction of radiative heat loss. The proposed concentrator exhibits high thermal performance even at high absorber temperatures.

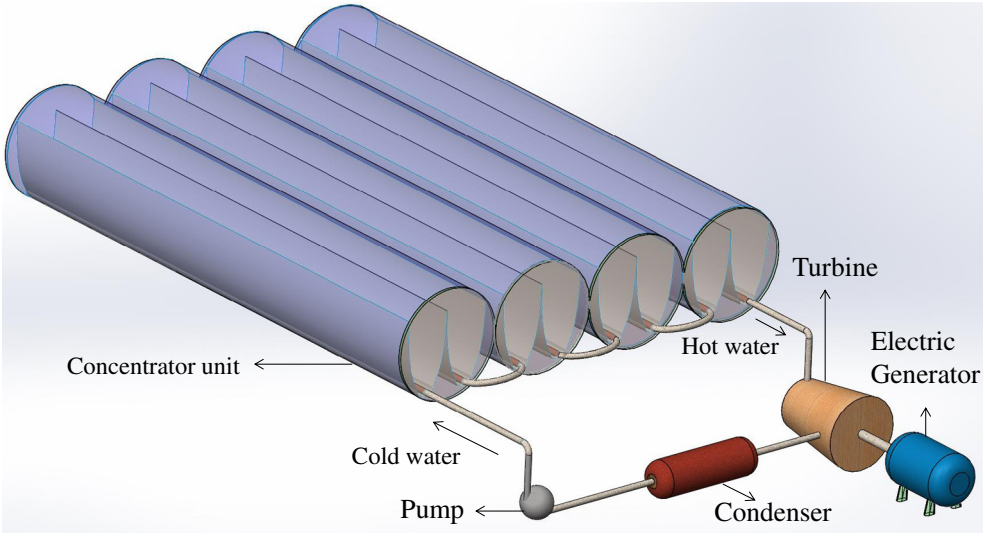

Fig. 17. Dual concentrator unit, Rankine cycle.

On the other hand, using a dual concentrator can help reduce the material cost for multiple concentrator applications due to a slight increase in the glass tube's size. Moreover, simulations suggest that ray acceptance is significantly increased; thereby, the performance is improved compared to a single concentrator and the same amount of energy as obtained from the single one can be achieved by using smaller projected area with smaller amount of glass material.

In addition, water flow in the absorber can be provided by using a U-Type pipe absorber for dual concentrator (Fig. 16). This type of absorber pipe can be supplied from the market and can be easily used in construction. Also note that only one end of the glass tube requires insulation to provide vacuum.

Seasonal and annual evaluations were also performed for the proposed concentrators. A calculation method was adapted for performance evaluation by using a 2-D ray tracing method. Dual concentrators performed better in seasonal and annual evaluations but may require seasonal adjustment of orientation. An alternative way to achieve longer heat generation without any orientation adjustment is to enhance the acceptance angle. This will increase the utilization time significantly, thus improving the performance. Furthermore, the manufacturing cost will be reduced due to a significant reduction of the reflector area and glass tube size. The proposed concentrator can be used for steam generation by using the optimal reflector and glass tube sizes that are available on the market in configuration of low heat loss and long-term durability (Fig. 17). All of these features encourage promoting the operation of dual concentrators. Additional evaluations will be conducted in future experimental studies.

4. Conclusions

In this study, the dual concentrator was compared with the single one to investigate the changes in optical and thermal performance. A calculation model was proposed to calculate the seasonal performance. Results are summarized as follows.

(1) Although two combined reflectors were used in the dual concentrator, a slight oversizing of 28% occurred on the circumference of the glass cover. Using the dual concentrator can reduce the manufacturing costs because of the relatively reduced glass cover area.
(2) In the case of dual concentrator, ray acceptance significantly increased, thereby enhancing the performance. In the case of normal incidence, only 52% of rays can enter the aperture of the single concentrator, while 82% of rays can enter the aperture of the dual concentrator. The average optical efficiency of the dual concentrator is about 57%, while that of the single one is 37%.
(3) When the absorber temperature is assumed to be 373 K, the single concentrator has the thermal efficiency of 12.6%, while the thermal efficiency of the dual concentrator reaches 33.63% for the gray surface absorber.
(4) The effect of selective coating on the performance of the proposed solar concentrator was also analyzed. The dual concentrator with selective coating absorber has average efficiency of 56% and the efficiency of the single one is 35%. When the absorber temperature is assumed to be 473 K, the dual concentrator with selective coating operates with the efficiency of 52.7% and the efficiency of the single one becomes 31%. Performance evaluation shows that the concentrators with selective surface absorber can be used with high efficiency in high temperature applications such as steam generation, because gray surface is suitable to attain hot water.
(5) Seasonal and annual performance evaluations show that the efficiency of the dual concentrator is better compared to that of the single one, as the efficiency varies depending on the angle of incidence and solar intensity. In general, the highest performance is observed at 12:00, resulting from higher solar heat flux as the efficiency slightly increases for angles of incidence that approach the maximal efficiency angle of 12°. In addition, the difference in the operating time is irrelevant judging by the day-time characteristic while the key element determining the performance is the value of the solar projection angle. A small seasonal adjustment in the orientation or an increase of the acceptance angle is needed for longer utilization of solar energy during early morning and late afternoon hours for the solstice and the days around it. Increasing the acceptance angle will improve the performance in connection with higher ray acceptance and optical performance, as the component cost will decrease due to a smaller reflector size.

References

Adsten M, Hellstorm B, Kalsson B. Measurement of radiation distribution on the absorber in a asymmetric CPC collector. Sol Energy 2004;76:199–206.
Balat M. Political, economic and environmental impacts of biomass based hydrogen. Int J Hydrog Energy 2009;34:3589–603.
Eames PC, Norton B. Validated, unified, model for optics and heat transfer in line-axis concentrating solar energy collectors. Sol Energy 1993;50-4:339–55.
Gudekar AS, Jadhav AS, Panse SV, Joshi JB, Pandit AB. Cost effective design of compound parabolic collector for steam generation. Solar Energy 2013;90:43–50.
Hinterberger H, Winston R. Efficient light coupler for threshold Cerenkov counters. Rev Sci Instrum 1966a;37:1094–5.
Hinterberger H, Winston R. Gas Cerenkov counter with optimized light-collecting efficiency. Proc. Int. Conf. Instrumentation High Energy Phys; 1966b. p. 205–6.
Hirasawa S, Tsubota R, Kawanami T, Shirai K. Reduction of heat loss from solar thermal collector by diminishing natural convection with high-porosity porous medium. Sol Energy 2013;97:305–13.
Howell JR, Bannerot RB, Vliet GC. Solar-thermal energy systems analyse and design. McGraw-hill; 1982. p. 22.
IEA (International Energy Agency). Technology roadmaps—solar photovoltaic energy. Paris, France: IEA; 2010.
Kalogirou AS. Solar thermal collectors and applications. Prog Energ Combust 2004;30(3): 231–95.
Kaltenbach T, Kurth M, Schmidt C, Meier T, Kohl M, Weib K. Aging test of components for solar thermal collector. Energy Procedia 2012;30:805–14.
Khoukhi M, Maruyama S. Theoretical approach of a flat plate solar collector with clear and low-iron glass covers taking into account the spectral absorption and emission within glass covers layer. Renew Energy 2005;30:1177–94.
Khoukhi M, Maruyama S, Komiya A, Behnia M. Flat-plate solar collector performance with coated and uncoated glass cover. Heat Transfer Eng 2006;27:46–53.
Kim Y, Han GY, Seo T. An evaluation on thermal performance of CPC solar collector. Int Commun Heat Mass 2008;35:446–57.
Maruyama S. Uniform isotropic emission from an aperture of a reflector. Proceedings Fourth ASME/JSME Joint Thermal Engineering Conference, Nevada; 1991.
Maruyama S. Uniform isotropic emission from an involute reflector. J Heat Trans-T ASME 1993;115(2):492–5.
Mcintire WR. New reflector design which avoids losses through gaps between tubular absorbers and reflectors. Sol. Energy 1980;25(3):215–20.
McIntire WR, Reed KA. Orientational relationships for optically non-symmetric solar collectors. 1983;31(4):405–10.
Nostell P, Roos A, Karlsson B. Ageing of solar booster reflector materials. Sol Energy Mater Sol Cells 1998;54:235–46.
Oommen R, Jayaraman S. Development and performance analysis of compound parabolic solar concentrators with reduced gap losses – oversized reflector. Energy Convers Manag 2001;42-11:1379–99.
Ouagued M, Khellaf A, Loukarfi L. Estimation of the temperature, heat gain and heat loss by solar parabolic trough collector under Algerian climate using different thermal oils. Energy Convers Manag 2013;75:191–201.
Pinazo JM, Canada J, Arago F. Analysis of the incident angle of the beam radiation on CPC. Sol Energy 1992;49(3):175–9.
Rabl A. Optical and thermal properties of compound parabolic concentrators. Sol Energy 1976a;18:497–511.
Rabl A. Comparison of solar concentrators. Sol Energy 1976b;18:93–111.
Snail K, Ogallagher JJ, Winston R. A stationary evacuated collector with integrated concentrator. Sol Energy 1984;33:441–9.
Solangi KH, Islam MR, Saidur R, Rahim NA, Fayaz H. A review on global solar energy policy. Renew Sustain Energy Rev 2011;15:2149–63.
Souliotis M, Tripanagnostopoulos Y. Study of the distribution of the absorbed solar radiation on the performance of a CPC-type ICS water heater. Renew Energy 2008;33: 846–58.
Su Y, Pei G, Riffat SB, Huang H. A novel lens-walled compound parabolic concentrator for photovoltaic applications. J Sol Energ-T ASME 2012;134.
Tabor H. Comment –the CPC concept, theory and practice. Sol Energy 1984;33:629–30.
Tian Y, Zhao CY. A review of solar collectors and thermal energy storage in solar thermal applications. Appl Energy 2013;104:538–53.
Topkaya SO. A discussion on recent developments in Turkey's emerging solar power market. Renew Sustain Energy Rev 2012;16:3754–65.

Tripanagnostopoulos Y, Yianoulis P, Papaefthimiou S, Zaferiatos S. CPC solar collector with flat bifacial absorbers. Sol Energy 1999;69-3:191–203.
Ustaoglu A, Okajima J, Zhang X, Maruyama S. Evaluation of an organic Rankine cycle using a non-imaging solar concentrator for different working fluids. Acad Platform J Eng Sci 2015a;2015(3–3):1–7. http://dx.doi.org/10.5505/apjes.2015.18209.
Ustaoglu A, Okajima J, Zhang X, Maruyama S. Performance evaluation of a proposed solar concentrator In terms of optical and thermal characteristic. Environ Prog Sustainable Energy 2015b. http://dx.doi.org/10.1002/ep.12236.

Nomenclature

A_c *Aperture area of the concentrator (m^2):*
A_a *Receiver area of CPC, absorber surface area (m^2):*
C *Concentration ratio (—):*
I_{in} *Solar beam intensity (W/m^2):*
n *Number of rays captured along with the concentrator's aperture area (—):*
Nr *Number of rays (—):*
R_{loss} *Ray loos from sides of concentrator:*
Rn *Number of reflection before reaching the absorber (—):*
T_a *Average absorber temperature (K):*
T_{amb} *Maximum absorber temperature (K):*
T_c *Average glass cover temperature (K):*
q_s *Solar insolation (W/m^2):*
q_r *Radiative heat loss (W):*
q_c *Convective heat loss (W):*
U *Overall heat transfer coefficient ($W/m^2 \cdot K$):*

Greek symbols

α_a *Solar altitude angles for summer solstice (dgr):*
α_b *Solar altitude angles for winter solstice (dgr):*
α_{ab} *Absorptivity of absorber:*
α_s *Solar altitude:*
β *Tilt angle of concentrator:*
γ_s *Solar azimuth angle:*
γ_c *Surface azimuth angle:*
δ *Declination:*
ε *Emissivity of absorber:*
η_{opt} *Optical efficiency:*
η_{th} *Thermal efficiency:*
θ *Incident angle of ray in 2D calculation:*
θ_{3D} *Incident angle of oblique ray in 3D geometry:*
θ_{2D} *Projection of θ_{3D} in 2D surface:*
θ_{max} *Maximum acceptance angle:*
ρ_r *Reflectivity of the reflector:*
σ *Stefan Boltzman constant:*
τ_c *Transmissivity of the glass tube:*
ϕ *Latitude:*
ω *Hour angle:*